



HAL
open science

Estimation of external contact loads using an inverse dynamics and optimization approach: general method and application to sit-to-stand maneuvers.

Thomas Robert, Julien Causse, Gérard Monnier

► To cite this version:

Thomas Robert, Julien Causse, Gérard Monnier. Estimation of external contact loads using an inverse dynamics and optimization approach: general method and application to sit-to-stand maneuvers.. Journal of Biomechanics, 2013, 46 (13), 2220-2227 pp. 10.1016/j.jbiomech.2013.06.037 . hal-02072691

HAL Id: hal-02072691

<https://hal.science/hal-02072691>

Submitted on 19 Mar 2019

HAL is a multi-disciplinary open access archive for the deposit and dissemination of scientific research documents, whether they are published or not. The documents may come from teaching and research institutions in France or abroad, or from public or private research centers.

L'archive ouverte pluridisciplinaire **HAL**, est destinée au dépôt et à la diffusion de documents scientifiques de niveau recherche, publiés ou non, émanant des établissements d'enseignement et de recherche français ou étrangers, des laboratoires publics ou privés.

Estimation of external contact loads using an inverse dynamics and optimization approach: general method and application to sit-to-stand maneuvers.

T. Robert^{a,*}, J. Causse^{a,b}, G. Monnier^{a,c}

^a*Université de Lyon, F-69622, Lyon, France
IFSTTAR, LBMC, F-69675 Bron*

Université Lyon 1, LBMC, F-69373 Lyon

^b*PSA Peugeot-Citroen, France*

^c*In-Motion, France*

Abstract

This paper presents a general method to estimate unmeasured external contact loads (ECL) acting on a system whose kinematics and inertial properties are known. This method is dedicated to under-determinate problems, e.g. when the system has two or more unmeasured external contact wrenches. It is based on inverse dynamics and a quadratic optimization, and is therefore relatively simple, computationally cost effective and robust. Net joint loads (NJL) are included as variables of the problem, and thus could be estimated in the same procedure as the ECL and be used within the cost function.

The proposed method is tested on human sit-to-stand maneuvers performed holding an handle with one hand, i.e. asymmetrical movements with multiples external contacts. Three sets of measured and unmeasured contact load components and three cost functions are considered and simulated results are compared to experimental data. For the population and movement studied, better results are obtained for a least square sharing between actuated degrees of freedom of the relative motor torques (motor torques normalized by the maximal torque production capacity). Moreover, the number of unknown ECL components does not significantly influence the results. In particular, measuring only the vertical

*Corresponding author

Email address: `thomas.robert@ifsttar.fr` (T. Robert)

force under the seat lead to a relatively correct estimation of the ECL and NJT (RMS differences about 10 % and 20 % of the amplitude for the ECL and the NJT respectively), and to observe the influence of an experimental parameter (the Seat Height).

Keywords:

Inverse Dynamics, Under-determinate problem, External contact loads, Joint loads, Optimization, Sit to stand

1. Introduction

Human motion analysis focuses more and more on dynamic variables. In particular, analysis of the external contact loads (ECL) allows characterizing the nature and the role of interactions between a subject and its environment. For example, Chateauroux and Wang (2010) classified hand/vehicle contacts during car ingress/egress motions based on their role on the motion: exploration of the environment, balance maintenance and participation to the displacement.

Knowledge of the ECL is also necessary to analyze the dynamics of a motion, typically the internal loads such as the net joint torques (NJT) or muscle forces. These internal loads are not directly measurable with non invasive techniques. They are usually estimated using inverse dynamic approaches, i.e. based on the knowledge of the system's kinematics, its inertia properties and the ECL acting on it (e.g. Dariush et al., 2000; Doriot and Cheze, 2004; Dumas et al., 2007b; Silva and Ambrosio, 2002; Winter, 1990).

Classically ECL are directly recorded using load sensors. However, direct measurement may be technically complex, especially for ambulatory or "out of the lab" experiments. Besides, use of force sensors tends to reduce the "ecological" aspect of an experiment. A classical illustration would be the force plate targeting problem in gait analyses (Challis, 2001; Oggero et al., 1998). Another example would be ergonomic experiments performed in complex environments, such as car ingress-egress (Causse et al., 2009; Kim and Lee, 2009) where the difficulty to equip every mock-up parts lead experimenters to limit the possible contact areas for the subject, and eventually limit the variety and naturalness of movements.

It is therefore necessary to use modeling techniques to indirectly estimate the ECL from the known kinematics of body segments (measured or simulated). One of the method could be to use a detailed model of the contacts, in particular for the foot-ground contact during locomotion (Fluit et al., 2012; Pandy, 2001). However such models are difficult to adjust, potentially expensive in computation and sensitive to the modeling hypotheses (Dorn et al., 2012). An alternative

is to use an inverse approach, i.e. to estimate the ECL acting on a system that lead to its observed motion (Pillet et al., 2010; Sanders et al., 1991). However, one of the limitations of this approach is that it becomes under-determined if there are more unknown ECL components than independent governing equations. This usually occurs when there are multiple unmeasured contacts loads with the environment. Thus, setting an assumption on the load sharing becomes necessary.

In the past, only few studies have proposed to deal with these types of under-determined problems. Most of them focused on bipedal phase of the gait and represented the load sharing with mathematical functions (Davis and Cavanagh, 1993; Hardt and Mann, 1980; Koopman et al., 1995; Ren et al., 2008). While these methods provided satisfying results, they were very specific to the given task and the population. A more generic approach for solving the load sharing problem consists by minimizing a cost function was presented by (Vaughan et al., 1982). Instead of focusing only on the ECL problem, Vaughan et al. (1982) chose to explicitly introduce the unknown net joint loads (NJL) into the problem. It allowed to estimate NJL and ECL in the same procedure and also to use NJL into the cost function. Based on this approach, they obtained interesting results for different kind of movements. However, the study suffered from several limitation: there results were strongly dependent on the initial guess of the solution, the methods was only tested in 2D and in cases with no more than two unknown ECL wrenches, and the results were reported for only one cost function.

This indicates that there is still a lack of methodologies for estimating the ECL, particularly in under-determined cases. This study proposes a generic method which utilizes a combination of inverse dynamics and optimization. It is intended to be relatively simple, computationally cost effective and robust. The proposed method is tested on human sit-to-stand maneuvers performed holding an handle with one hand, i.e. asymmetrical movements with multiples external contacts. Influence of the number of unknown ECL components and of different cost functions are evaluated.

2. Modeling

This section introduces the generic problem to be solved in this study.

2.1. Description of system considered

65 The system considered is a whole body human model made of n_s rigid segments linked by n_j joints representing a total of n_{dof} degrees of freedom (DoF). The kinematics and inertia properties of the segments are considered to be known.

2.2. Dynamics and constraints of the system

70 The dynamic wrenches for each segments, due to the inertial and gravitational effects, can be estimated from their kinematics and inertia properties and aggregated to obtain the dynamic wrench of the overall system. This wrench has to be balanced by the known and unknown ECL, resulting in a system of 6 linear equations with n_u unknowns. Alternatively, we chose to write the
75 Newton-Euler equations for each segments, introducing the internal loads acting between the segments. It led to a set of $6n_s$ linear equations (6 per segments) with $n_u + 6n_j$ unknowns (corresponding to the unknown ECL components and the NJL):

$$a_{eq}x = b_{eq} \quad (1)$$

were $x = [S \ U]^t$ is a single vector grouping all the unknowns, S is the vectors
80 containing the $6n_j$ NJL (3 forces and 3 torques per joint), U is the vectors of the n_u unknown ECL components, a_{eq} is a matrix relating the joints and unknown ECL components with the corresponding affected segments, and b_{eq} is the effect of the dynamic wrench, known ECL and loads due to the gravity for all the segments (see Appendix for the details).

85 The physical limitations of the studied system, such as unilaterality of the contacts or maximum motor torques that could be developed, are also considered in this study. In order to make the resolution of the problem faster and more robust (see Section 2.3), we chose to express these limitations as linear equations

of the unknown vector x . Mathematical description of these constraints are
 90 given in Appendix.

The description of the system dynamics and limitations boils down to the linear system:

$$\begin{cases} a_{eq}x & = b_{eq} \\ a_c x & \leq b_c \end{cases} \quad (2)$$

2.3. Resolution

This study focuses on under-determined problems for which there are fewer
 95 governing equations than the unknowns ($6n_s < 6n_j + n_u$). In order to select only one solution among all the possibles, additional expectations for this solution are introduced via a function to be minimized. For numerical purposes (developed in the discussion) we propose: 1) to write this function in a specific form (squared euclidean norm of a linear function of x), 2) to add an additional term to it
 100 — the squared euclidean norm of x with a very low weighting factor — and 3) to set the equality constraints as penalties. Eventually, it led to the following optimization problem:

$$\min_x \alpha \|sx\|^2 + \beta \|x\|^2 + \gamma \|a_{eq}x - b_{eq}\|^2, \text{ s.t. } a_c x \leq b_c \quad (3)$$

where $\| \cdot \|$ represents the euclidean norm, s is a matrix defining a linear transformation of x , and α , β and γ are weighting factors.

105 This problem can be rewritten as a quadratic programming problem:

$$\min_x \frac{1}{2} x^T H x + g^T x, \text{ s.t. } a_c x \leq b_c \quad (4)$$

with $H = 2\alpha s^T s + \beta I + \gamma a_{eq}^T a_{eq}$ a positive definite matrix (see Discussion) and $g^T = -2\gamma b_{eq}^T a_{eq}$.

3. Case Study

3.1. Task and motions studied

110 Experimental data were collected on six healthy young male volunteers (stature = 1752 ± 61 mm, weight = 66 ± 8 kg and age = 26 ± 3 yo), having no musculoskeletal disorder.

Subjects were initially seated on a flat rigid seat with feet on the ground and the right hand grasping a horizontal handle. The handle was centered in
115 the sagittal plane of the subject, located at the level of the subject's eyes when seated and at a distance corresponding to the shoulder-wrist length. They were asked to rise from the seat to a standing posture using the handle (see Figure 1). Three different seat heights were tested: 50% (H_{50}), 75% (H_{75}) or 100% (H_{100}) of the knee height. The task was repeated two times for H_{50} and H_{100}
120 and six times for H_{75} .

3.2. Experimental Data Collection and Processing

A Motion Analysis[®] system, sampling at 100Hz, was used to capture the trajectories of 51 reflective markers placed on the subject. All ECL between the subject and its environment were recorded using three force plates (under each
125 foot and under the seat) and a 6-axes load sensor placed between the handle and the frame.

Kinematics was reconstructed using a global optimization procedure (Wang et al., 2005) and a 16 rigid bodies - 33 degrees of freedom kinematic model (see Figure 2). The segment inertia parameters were estimated from regression equations (Dumas et al., 2007a). NJL were computed using a recursive
130 approach (Doriot and Cheze, 2004) and two calculation strategies (bottom-up and top-down) converging at the lumbar joint (Robert et al., 2007). These NJL computed using all the contact loads information will later be used as reference to estimate the quality of the optimization (see Section 3.5).

135 *3.3. Modeling Hypotheses*

The methodology proposed in section 2 is applied using the measured kinematics and different subsets of the measured ECL.

Three different sets of known (i.e. which are measured) and unknown ECL were considered (see Figure 2): 1) S_1 - both seat and hand contact wrenches are
140 known; 2) S_2 - only seat contact wrench is known; 3) S_3 - only the vertical force of seat contact wrench is known and other components are assumed absent.

When unknown, hand to handle interaction was represented by a full wrench applied at the projection of the third metacarpophalangeal joint on the handle. The contact between the foot and the ground were modeled as 3 punctual unilat-
145 eral contacts with tangential force limited by friction (static coefficient $\mu=0.5$) and positioned under the 1st and the 5th metatarsal heads and the heel. These 3 punctual contact wrenches were further aggregated to represent the foot to ground interaction with a single contact wrench.

Figure 2 about here.

150 Three types of constraints were applied: unilaterality and dry friction constraints for punctual contacts, and maximal motor torques that could be developed by the subject (see Table 1). Mathematical description of these constraints are given in Appendix.

Table 1 about here.

155 *3.4. Resolution of the Optimization Problem*

Three different expectations on the load sharing were tested: minimization in a least square sense of 1) the unknown external contact forces (ECF); 2) the net joint torques (NJT), 3) the motor torques normalized by their maximum allowable value (MT_% see Table 1). It resulted in three cost functions C_i 's of
160 the form:

$$C_i(x) = \alpha_i \|s_i x\|^2 + \beta \|x\|^2 + \gamma \|a_{eq} x - b_{eq}\|^2 \quad (5)$$

with s_i matrices defining the linear transformation of x — the unknown vector of ECL and NJL — into the vector of ECF, NJT or $MT_{\%}$ respectively (details in Appendix). Values of α_i were adjusted based on the average value of s_i (see Table 2), while β and γ were set to 10^{-5} and 10^5 respectively.

165 These quadratic programming problems were solved using the Matlab[®] *quadprog* solver. The algorithm was automatically initialized for the first frame of the motion (initial point set to a vectors of ones (MathWorks, 2012)). For the remaining frames it was initialized using the results of the previous frame.

3.5. Analyses

170 Three cost functions ($C_1 - C_3$), three contact configurations ($S_1 - S_3$) and three experimental seat heights (H_{50} , H_{75} and H_{100}) were considered. Seven combinations of these variables were tested (see Table 2). For each of them, the NJL and the unknown ECL were estimated for every maneuver performed by the six subjects. Forces and torques were normalized by body weight (BW) and body weight times body height (BW.BH) respectively (Hof, 1996). Peak values of the norm of the simulated ECL and NJT were extracted and referred as P_{sim} hereafter. In addition, time history profiles of the norm of the simulated data were compared to their reference curves. RMS differences normalized by the amplitude of the reference curve were computed and referred as $R_{\%}$. The 175 reference data were: 1) the measured experimental data for the ECL; 2) the results of the inverse dynamics performed using the experimentally measured ECL (see section 3.2) for the NJT.

ANOVAs and Tukey's post-hoc tests were used to analyze the effects of 1) the cost function on $R_{\%}$ in S_2 and H_{75} (three first rows of Table 2), 2) the 185 contact configuration on $R_{\%}$ using C_3 and in H_{75} (rows three to six of Table 2), and 3) the seat height on P_{sim} using C_3 and in S_3 (last three rows of Table 2).

4. Results

The procedure successfully converged for all the tested motions and configurations. An evaluation was performed to observe if equality constraints set as

190 penalties were satisfied. It was found that the residual values of $\|a_{eq}.x - b_{eq}\|^2$
(see Equation (5)) remained negligible (less than 10^{-4}) in all cases, except for
some motions in contact the configuration S_1 , where it reached up to 3 N.m
around the seat-off for torque constraints along the transverse axis.

Figure 3 displays an example of reference data (measured ECL and NJT
195 obtained through inverse dynamics with the measured ECL) for a representative
subject in configuration S_2 and H_{75} . These results are comparable in term of
profiles and amplitude to the classical data available in the literature for sit-
to-stand maneuver (Bahrami et al., 2000; O’Meara and Smith, 2006). In this
Figure 3, simulated results obtained in the same situation for different cost
200 functions are also superimposed to the reference data. Both the shape of the
simulated curves and their amplitudes are overall in good agreement with the
reference ones.

An example of simulated and measured center of pressure trajectories under
each foot is shown in Figure 4. The loaded area are comparable. In this partic-
205 ular case the experimental trajectory goes outside the modeled base of support
(BoS) for some frames of the motion, whereas the simulated trajectory remains
inside.

Figure 5 displays the normalized RMS differences between the simulated and
reference data ($R_{\%}$) averaged accross trials and subjects for each contact and
210 joints and the three cost functions tested (contact configuration S_2 and seat
height H_{75}). Very high values for the right wrist NJT are due to very small
amplitudes of the reference curves. Therefore, they are discarded in further
analyses. Overall, $R_{\%}$ are smaller for C_3 and higher for C_1 . This is confirmed by
an ANOVA with factors *Contact* and *Cost function* performed on the $R_{\%}$ values
215 of the ECF. It showed a significant effect ($p < 0.05$) of the *Cost function*, the
Contact and their interactions. Post-hoc tests showed that $R_{\%}$ are significantly
different for each cost function, with the smallest values for C_3 and the highest
for C_1 . Similar results are obtained for the NJT, although $R_{\%}$ for C_2 and C_3
are not significantly different.

220 A similar analysis was performed to evaluate the effect of the contact config-

uration using the cost function C_3 in seat height H_{75} . An ANOVA with factors *Contact* and *Contact configuration* performed on the $R\%$ for the ECF showed that neither the *Contact configuration* nor the interaction has a significant effect ($p = .157$ and $p = .321$, respectively). Similar results are obtained for the NJT.

225 Two ANOVAs with factors *Contact* and *Seat height* performed on the P_{sim} for the ECF and for the NJT confirmed that the *Seat height* has a significant effect on the P_{sim} . Post-Hoc tests showed that the higher the seat the smaller the P_{sim} ($H_{100} < H_{75} < H_{50}$).

5. Discussion

230 5.1. Numerical Aspects

This paper presents a general method to estimate unmeasured external contact loads acting on a system whose kinematics and inertial properties are known. This method was intended to be relatively simple and robust. For the case study considered the optimization problem converged systematically, and one could remark the smoothness of the time profile for the simulated variables, although the problem is solved frame by frame. It is notably imputable 235 to the numerical properties of the optimization problem. We chose to write the problem as a quadratic program (quadratic cost function and linear constraints). For this type of problem, if the H matrix of the cost function (see equation 5) is positive definite (always non negative, nil only for $x = 0$) and if 240 the problem has a solution, then it exists a unique minimum that is the global minimum. The solver will thus systematically and quickly converge toward the desired solution.

The cost functions used in this study are the sum of three terms (see Equation (5)). The first and last terms are strictly non negative functions that may 245 be equal to zero for non zero value of x . Adding the squared norm of x , even with a very small weight, ensures that the cost function can only be nil only when $x = 0$, i.e. the cost functions are positive definite. In other words, the first and last terms of the cost function did not necessarily nullify the space of

250 solution. Typically the foot contact model used in this study (3 contact points) induced a redundancy in the horizontal plane: an infinity of individual contact forces combinations summed up to the same overall contact force for the foot, and thus the same motor torques and the same value of the optimization criterion. The role of the second part of the criterion, slightly weighted, is then
255 to nullify the space of solution and as such to improve the stability and convergence efficiency of the optimization algorithm. Because of its small relative weight, it did not significantly changed the results in terms of the resultant of ECL or NJL.

This study focused on under-determined problems. However, in some situations, the system of equation (2) may become over-constrained. It typically
260 happens in case of temporary inconsistencies between the modeling hypotheses and the imposed experimental data (estimated accelerations or BSIP). In this study we chose to set the equality constraints as penalties in the cost function. It led to the optimization problem (3), only constrained by the set of inequalities representing the system's limitations. These later are independent of the
265 experimental data and, besides modeling incoherences, unlikely to nullify the space of solution. Consequently the problem (3) always has at least a solution. Although this solution only satisfies as well as possible the equations of motion, it may be acceptable for small residual values of the penalties. In this study
270 over-constrained situations may happen around the seat-off in the contact configuration S_1 . As displayed in Figure 4, the foot contact wrenches may be too tightly constrained for some motion, leading to small discrepancies between the modeled BoS and the experimental CoP trajectory. These discrepancies could be compensated by the hand contact wrench when this later is not imposed, but
275 led to an over-constrained problem when the hand contact wrench is imposed (contact configuration S_1). The observed residual values remained relatively small, and the obtained solutions were thus acceptable. However, a track for improvement would be to finely defined the shape of the BoS, by adding contact points for example.

280 5.2. Case study: cost function and applicability

The proposed methodology was applied to sit-to-stand motions with an handle. Different load sharing hypotheses were tested. Cost function C_3 provide the better results (the smaller $R\%$). It principally implies a least square sharing between actuated DoF of the relative motor torques (motor torques normalized
285 by the maximal torque production capacity). It therefore prevents to overload those DoF which are having small capacity. This effect is best seen on the right upper limb, where the use of C_3 tend to limit the loads along the right upper limb DoF, with smaller force production capacities relative to those of the lower limbs. This criterion is quite similar to the minimization of the individual
290 muscle stress (individual muscle forces normalized by their physiological cross sectional area) classically used for solving the under-determined muscle force sharing problem (e.g. Erdemir et al., 2007, for a review). Other criteria could have been considered, in particular considering the p-norm of $s_i x$ to the power p with $p \neq 2$ and the min/max criterion (Rasmussen et al., 2001). It could also
295 be interesting to extend this problem to include individual muscle forces in the criterion. It would not change the nature of the problem as, by neglecting the contraction dynamics, the muscle forces can be expressed as a linear function transformation of the motor torques via a level arm matrix.

Three different contact configurations were considered in this study. Sta-
300 tistical analysis showed that this parameter did not significantly influence the quality of the results (difference between reference and simulated data). In particular, reducing the number of unknowns did not improve the $R\%$ (S_1 vs S_2). Results obtained in S_3 (using only the vertical force component of the seat contact wrench) are important in terms of application. They suggest that, for the
305 studied movement and population, measuring only the vertical force under the seat would allow a relatively correct estimation of all ECL and NJT: not only the values of $R\%$ were small (about 10% for the feet ECL and 20 % for the NJT), but the influence of an experimental parameters (the Seat Height) was also correctly predicted. In this case, peak values of NJT and ECL increased when the seat
310 height decreased, as observed from the experimental data (Robert et al., 2011).

This could be of particular importance for ergonomic studies where usually the goal is to understand the influence of different experimental parameters on the motion dynamics and which often suffer from instrumentation difficulties.

5.3. Limitations

315 The methodology was only evaluated for one type of motion and a small sample of single population. Load sharing criterion may evolve between motion and population, and may include other parameters such as the comfort or balance. This should be further studied.

320 Moreover, the contact configurations considered in this study remained constant during the motion. Although the kinematics and measured contact loads may sufficiently drive the problem, discontinuities in solution may appear when considering intermittent contacts. One could thus consider describing the problem using parametric curves and to solve it as a whole instead of frame by frame.

325 Conflict of interest statement

None of the authors has any conflict of interest to report in this research.

Bahrami, F., Riener, R., Jabedar-Maralani, P., Schmidt, G., 2000. Biomechanical analysis of sit-to-stand transfer in healthy and paraplegic subjects. *Clinical Biomechanics* 15, 123 – 133.

Causse, J., Chateauroux, E., Monnier, G., Wang, X., Denninger, L., 2009. Dynamic analysis of car ingress/egress movement: an experimental protocol and preliminary results. *SAE International Journal of Passenger Cars-Mechanical Systems* 2, 1633–1640.

Chaffin, D., Andersson, G., Martin, B., 2006. *Occupational Biomechanics*. J. Wiley & Sons, New York, NY. 4th edition.

Challis, J.H., 2001. The variability in running gait caused by force plate targeting. *Journal of Applied Biomechanics* 17, 77–83.

- Chateauroux, E., Wang, X., 2010. Car egress analysis of younger and older drivers for motion simulation. *Applied Ergonomics* 42, 169 – 177.
- Dariush, B., Hemami, H., Parnianpour, M., 2000. A well-posed, embedded constraint representation of joint moments from kinesiological measurements. *Journal of biomechanical engineering* 122, 437–445.
- Davis, B.L., Cavanagh, P.R., 1993. Decomposition of superimposed ground reaction forces into left and right force profiles. *Journal of Biomechanics* 26, 593 – 597.
- Delp, S.L., 1990. Surgery simulation: a computer graphics system to analyze and design musculoskeletal reconstructions of the lower limb. Ph.D. thesis. Stanford University.
- Doriot, N., Cheze, L., 2004. A three-dimensional kinematic and dynamic study of the lower limb during the stance phase of gait using an homogeneous matrix approach. *IEEE Trans Biomed Eng* 51, 21–27.
- Dorn, T.W., Lin, Y.C., Pandy, M.G., 2012. Estimates of muscle function in human gait depend on how foot-ground contact is modelled. *Computer Methods in Biomechanics and Biomedical Engineering* 15, 657–668.
- Dumas, R., Cheze, L., Verriest, J.P., 2007a. Adjustments to mcconville et al. and young et al. body segment inertial parameters. *Journal of Biomechanics* 40, 543–553.
- Dumas, R., Nicol, E., Cheze, L., 2007b. Influence of the 3D inverse dynamic method on the joint forces and moments during gait. *Journal of Biomechanical Engineering* 129, 786–790.
- Erdemir, A., McLean, S., Herzog, W., van den Bogert, A.J., 2007. Model-based estimation of muscle forces exerted during movements. *Clin Biomech (Bristol, Avon)* 22, 131–154.

- Fluit, R., van der Krogt, M., van der Kooij, H., Verdonschot, N., Koopman, H., 2012. A simple controller for the prediction of three-dimensional gait. *Journal of Biomechanics* 45, 2610 – 2617.
- Garner, B., Pandy, M., 2000. Musculoskeletal model of the upper limb based on the visible human male dataset. *Computer methods in Biomechanics and Biomedical Engineering* 4, 93–126.
- Hardt, D.E., Mann, R.W., 1980. A five body - three dimensional dynamic analysis of walking. *Journal of Biomechanics* 13, 455 – 457.
- Hof, A.L., 1996. Scaling gait data to body size. *Gait & Posture* 4, 222 – 223.
- Kim, S., Lee, K., 2009. Development of discomfort evaluation method for car ingress motion. *International Journal of Automotive Technology* 10, 619–627. 10.1007/s12239-009-0073-6.
- Koopman, B., Grootenboer, H.J., de Jongh, H.J., 1995. An inverse dynamics model for the analysis, reconstruction and prediction of bipedal walking. *Journal of Biomechanics* 28, 1369 – 1376.
- MathWorks, 2012. Optimization toolbox user's guide, matlab r2012b.
- Oggero, E., Pagnacco, G., Morr, D., Simon, S., Berme, N., 1998. Probability of valid gait data acquisition using currently available force plates. *Biomedical sciences instrumentation* 34, 392–397.
- O'Meara, D.M., Smith, R.M., 2006. The effects of unilateral grab rail assistance on the sit-to-stand performance of older aged adults. *Human Movement Science* 25, 257 – 274.
- Pandy, M., 2001. Computer modeling and simulation of human movement. *Annual review of biomedical engineering* 3, 245–273.
- Pillet, H., Bonnet, X., Lavaste, F., Skalli, W., 2010. Evaluation of force plate-less estimation of the trajectory of the centre of pressure during gait. comparison of two anthropometric models. *Gait & Posture* 31, 147–152.

- Rasmussen, J., Damsgaard, M., Voigt, M., 2001. Muscle recruitment by the min/max criterion – a comparative numerical study. *J Biomech* 34, 409–415.
- Ren, L., Jones, R.K., Howard, D., 2008. Whole body inverse dynamics over a complete gait cycle based only on measured kinematics. *J Biomech* 41, 2750–2759.
- Robert, T., Causse, J., Wang, X., 2011. Dynamics of sit-to-stand motions: effect of seat height, handle use and asymmetrical motions. *Computer Methods in Biomechanics and Biomedical Engineering* 14, 191–192.
- Robert, T., Chêze, L., Dumas, R., Verriest, J.P., 2007. Validation of net joint loads calculated by inverse dynamics in case of complex movements: application to balance recovery movements. *Journal of Biomechanics* 40, 2450–2456.
- Sanders, R.H., Wilson, B.D., Jensen, R.K., 1991. Accuracy of derived ground reaction force curves for a rigid link human body model. *Journal of Applied Biomechanics* 7, 330–343.
- Silva, M., Ambrosio, J., 2002. Kinematic data consistency in the inverse dynamic analysis of biomechanical systems. *Multibody System Dynamics* 8, 219–239.
- Vaughan, C.L., Hay, J.G., Andrews, J.G., 1982. Closed loop problems in biomechanics. part ii—an optimization approach. *J Biomech* 15, 201–210.
- Wang, X., Chevalot, N., Monnier, G., Ausejo, S., Ángel Suescun, Celigüeta, J., 2005. Validation of a model-based motion reconstruction method developed in the realman project. *SAE Transactions Journal of Passenger Cars - Electronic and Electrical Systems* 114, 873–879.
- Winter, D., 1990. *Biomechanics and Motor Control of Human Movement*. Wiley, New York.

Table 1

Table 1: Maximum torques for the different degrees of freedom of the considered model

Joint	Motion	Maximum torque value (N.m)	Source
Hip Joint	Flexion	185	Chaffin et al. (2006)
	Extension	190	Chaffin et al. (2006)
	Abduction	190	Delp (1990)
	Adduction	190	Delp (1990)
	Internal Rotation	60	Delp (1990)
	External Rotation	60	Delp (1990)
Knee Joint	Flexion	100	Chaffin et al. (2006)
	Extension	168	Chaffin et al. (2006)
	Internal Rotation	20	Expertize
	External Rotation	20	Expertize
Ankle Joint	Dorsiflexion	126	Chaffin et al. (2006)
	Plantarflexion	126	Chaffin et al. (2006)
	Inversion	20	Expertize
	Eversion	20	Expertize
Shoulder Joint	Flexion	92	Chaffin et al. (2006)
	Extension	67	Chaffin et al. (2006)
	Abduction	71	Chaffin et al. (2006)
	Adduction	67	Chaffin et al. (2006)
	Internal Rotation	52	Chaffin et al. (2006)
	External Rotation	33	Chaffin et al. (2006)
Elbow Joint	Flexion	77	Chaffin et al. (2006)
	Extension	46	Chaffin et al. (2006)
	Pronation	15	Garner and Pandy (2000)
	Supination	15	Garner and Pandy (2000)
Wrist Joint	Flexion	185	Garner and Pandy (2000)
	Extension	190	Garner and Pandy (2000)
	Abduction	190	Garner and Pandy (2000)
	Adduction	190	Garner and Pandy (2000)
Lumbar Joint	Flexion	143	Chaffin et al. (2006)
	Extension	234	Chaffin et al. (2006)
	Lateral Flexion	159	Chaffin et al. (2006)
Neck Joint	Flexion	100	Chaffin et al. (2006)
	Extension	100	Chaffin et al. (2006)

Table 2

Table 2: The different combination of parameters tested, and the corresponding weights of the cost function.

#	Cost Function	Contact Configuration	Seat Height	α_i	β	γ	Tested Effect
1	C_1	S_2	H_{75}	10^{-1}	10^{-5}	10^5	Cost Function
2	C_2	S_2	H_{75}	1	10^{-5}	10^5	
3	C_3	S_2	H_{75}	500	10^{-5}	10^5	
4	C_3	S_1	H_{75}	500	10^{-5}	10^5	Contact Configuration
3	C_3	S_2	H_{75}	500	10^{-5}	10^5	
5	C_3	S_3	H_{75}	500	10^{-5}	10^5	
6	C_3	S_3	H_{50}	500	10^{-5}	10^5	Seat Height
5	C_3	S_3	H_{75}	500	10^{-5}	10^5	
7	C_3	S_3	H_{100}	500	10^{-5}	10^5	

Figure 1

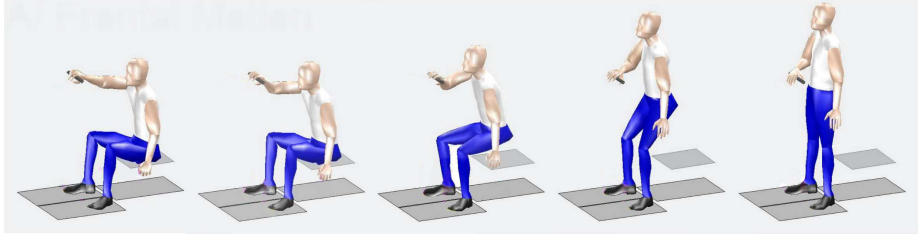


Figure 1: The sit to stand maneuver considered: example of a reconstructed motion with the seat height at 75% of the knee height.

Figure 2

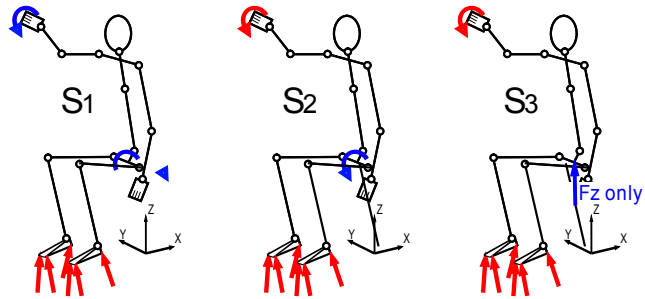


Figure 2: The multibody model considered in the three contact configurations tested. Straight and curved arrows stand for forces and full wrench respectively, whereas blue and red colors stand for known and unknown contact loads respectively.

Figure 3

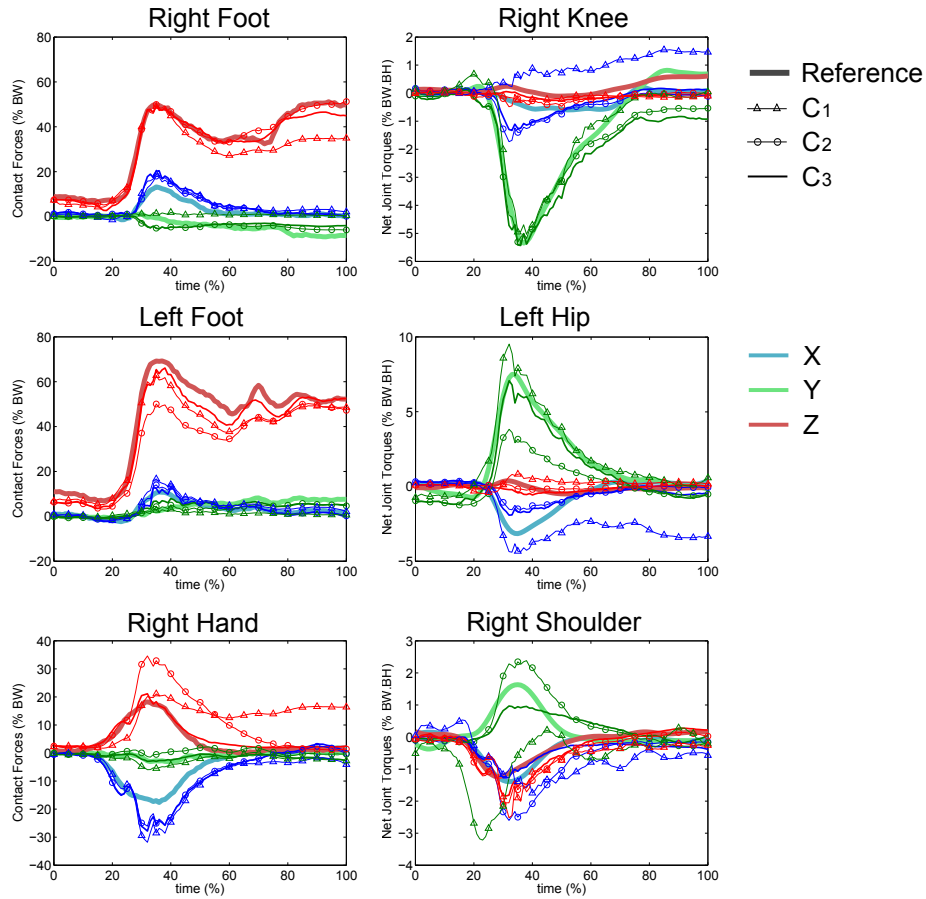


Figure 3: Example of reference and simulated contact forces and joint torques obtained for a sit-to-stand motion (seat height at 75% of the knee height, contact configuration S_2) for three different cost functions. Data are expressed in coordinate systems parallel to the Global Coordinate System. Differences among the cost functions are best seen for hand forces and shoulder torques(see last row in the figure).

Figure 4

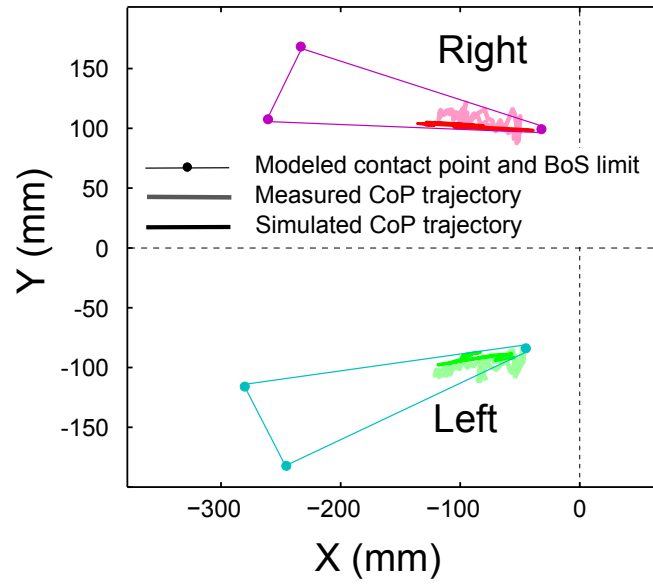


Figure 4: An example of the measured and simulated trajectories of the Center of Pressure under each foot, expressed in the global coordinate system. Note that in this case the experimental trajectories go out of the modeled base of support, while the simulated trajectories remain inside.

Figure 5

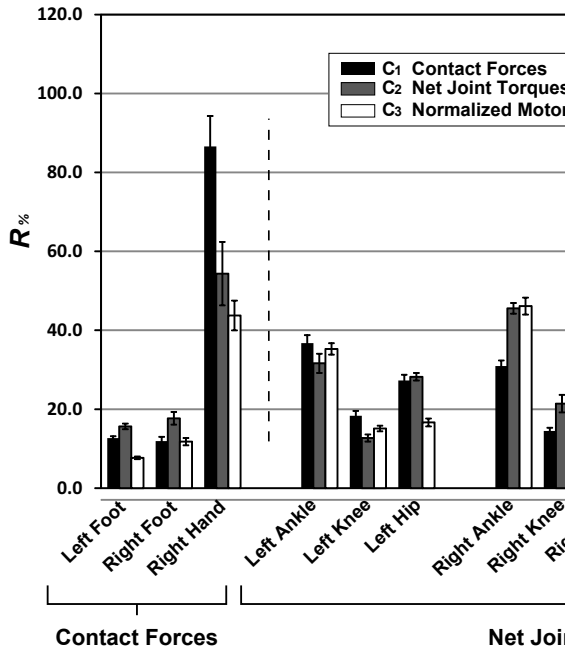


Figure 5: $R_{\%}$ (normalized RMS differences between simulated and reference data - see section 3.5) for different cost functions and different joint and contacts, averaged across subjects and trials, in contact configuration S_2 and seat height H_{75} . Vertical bars represents \pm one standard error of the mean (SEM). Results above 120% are given in the figure. The high values for the right wrist net joint torques are due to small amplitudes of the experimental curves.